APPLIED AND ENVIRONMENTAL MICROBIOLOGY, Mar. 2003, p. 1511–1520 Vol. 69, No. 3
0099-2240/03/$08.00+0 DOI: 10.1128/AEM.69.3.1511–1520.2003
Copyright © 2003, American Society for Microbiology. All Rights Reserved.

Bioaugmentation as a Tool To Protect the Structure and Function of an Activated-Sludge Microbial Community against a 3-Chloroaniline Shock Load

Nico Boon, Eva M. Top,† Willy Verstraete,* and Steven D. Siciliano‡

Laboratory of Microbial Ecology and Technology (LabMET), Ghent University, B-9000 Ghent, Belgium

Received 22 July 2002/Accepted 27 November 2002

Bioaugmentation of bioreactors focuses on the removal of xenobiotics, with little attention typically paid to the recovery of disrupted reactor functions such as ammonium-nitrogen removal. Chloroanilines are widely used in industry as a precursor to a variety of products and are occasionally released into wastewater streams. This work evaluated the effects on activated-sludge reactor functions of a 3-chloroaniline (3-CA) pulse and bioaugmentation by inoculation with the 3-CA-degrading strain *Comamonas testosteroni* I2 *gfp*. Changes in functions such as nitrification, carbon removal, and sludge compaction were studied in relation to the sludge community structure, in particular the nitrifying populations. Denaturing gradient gel electrophoresis (DGGE), real-time PCR, and fluorescent in situ hybridization (FISH) were used to characterize and enumerate the ammonia-oxidizing microbial community immediately after a 3-CA shock load. Two days after the 3-CA shock, ammonium accumulated, and the nitrification activity did not recover over a 12-day period in the nonbioaugmented reactors. In contrast, nitrification in the bioaugmented reactor started to recover on day 4. The DGGE patterns and the FISH and real-time PCR data showed that the ammonia-oxidizing microbial community of the bioaugmented reactor recovered in structure, activity, and abundance, while the number of ribosomes of the ammonia oxidizers in the nonbioaugmented reactor decreased drastically and the community composition changed and did not recover. The settleability of the activated sludge was negatively influenced by the 3-CA addition, with the sludge volume index increasing by a factor of 2.3. Two days after the 3-CA shock in the nonbioaugmented reactor, chemical oxygen demand (COD) removal efficiency decreased by 36% but recovered fully by day 4. In contrast, in the bioaugmented reactor, no decrease of the COD removal efficiency was observed. This study demonstrates that bioaugmentation of wastewater reactors to accelerate the degradation of toxic chlorinated organics such as 3-CA protected the nitrifying bacterial community, thereby allowing faster recovery from toxic shocks.

The main purpose of a wastewater treatment plant is to convert the organics present in an incoming wastewater stream to N_2 and CO_2 as well as to reduce the amount of suspended solids entering the environment. The biological treatment of industrial wastewaters by mixed microbial communities is, however, often disrupted by organic (e.g., chlorinated organics, phenolic compounds, surfactants, and herbicides) and inorganic (e.g., heavy metals, sulfides, and ammonia) chemicals present in the wastewater stream (7, 52). This disruption of biological processes results in inhibited nitrification, decreased carbon removal, and modification of sludge compaction properties (7, 29). Little is known about the composition of mixed microbial communities in reactors when biological processes are disrupted by or recovering from xenobiotic shocks. Most investigators focus on xenobiotic degradation, but in terms of the day-to-day functioning of the reactors, the restoration of biological activity such as ammonia removal is of primary importance.

The first and most critical step in the conversion of incoming ammonium to nitrogen is performed by a defined subgroup of bacteria, i.e., the ammonia-oxidizing bacteria (AOB). The removal of heterogeneous carbon from the wastewater stream is performed by diverse heterotrophic bacterial populations dominated by *Proteobacteria* (59). Sludge bulking, leading to suspended solids entering the environment, is a serious problem in 40 to 50% of all activated-sludge plants and is associated with large numbers of filamentous bacteria in the mixed liquor (58). The community composition of these diverse functional groups can be assessed by analysis of 16S rRNA (8, 38, 59) and genes involved in metabolic activities, such as ammonium monooxygenase (28, 31, 35). While analysis of the microbial community structure of bioreactors is typically based on the diversity of the pool of 16S rRNA genes, this DNA is very stable and its concentration is not correlated with cell activity. Therefore, DNA-based fingerprints only give an idea of the most abundant cells, either active, dormant, or dead, not necessarily of the most active ones. In contrast, since the number of rRNA copies per cell is proportional to cell growth rate (5) and thus to cell activity, fingerprint patterns based on rRNA better represent the most abundant as well as the highly active populations. In addition, fluorescent in situ hybridization (FISH) and real-time PCR on 16S rRNA with specific probes

* Corresponding author. Mailing address: Laboratory of Microbial Ecology and Technology (LabMET), Faculty of Agricultural and Applied Biological Sciences, Ghent University, Coupure Links 653, B-9000 Ghent, Belgium. Phone: 32 (0)9 264 59 76. Fax: 32 (0)9 264 62 48. E-mail: Willy.Verstraete@rug.ac.be.

† Present address: Department of Biological Sciences, University of Idaho, Moscow, ID 83844-3051.

‡ Present address: Department of Soil Science, University of Saskatchewan, Saskatoon, Saskatchewan S7N 5A8, Canada.

Downloaded from http://aem.asm.org/ on October 23, 2019 by guest

and primers allow changes in the number of active cells and rRNA copies under study, respectively, to be monitored.

The restoration of activity in wastewater treatment plants is a time-consuming and costly process. Many wastewater treatment plants contain buffering tanks or specialized microbial strains to protect the plant from a variety of chemical shocks (20), but there is no known process to specifically protect reactors from chloroaniline (CA) shocks. CAs are released during the production of polyurethanes, rubber, azo-dyes, drugs, photographic chemicals, varnishes, and pesticides (23, 33). The effect of CA on activated-sludge microbial communities is not known, but the nonchlorinated compound aniline inhibits nitrification (22, 29). We hypothesized that 3-CA shock loads in wastewater treatment plants will have a negative impact on wastewater treatment processes. The spontaneous removal of aromatic pollutants proceeds slowly and, in reactors, is not rapid enough to prevent reactor upset. In our previous work, a 3-CA-degrading strain, *Comamonas testosteroni* I2, was isolated from activated sludge, marked with the *gfp* gene, and used in a semicontinuous activated-sludge (SCAS) system to biodegrade a continuous stream of 3-CA-contaminated wastewater. For more than 14 days, strain I2 *gfp* removed all 3-CA (10, 12). Although strain I2 *gfp* was never tested in a wastewater treatment system where a shock load had occurred, we used it in this work I2 *gfp* to protect SCAS reactors from 3-CA shocks.

Few reports have investigated the recovery of disrupted reactor functions after bioaugmentation. Therefore, the aim of this work was to evaluate the short-term effects of a 3-CA shock load and bioaugmentation with a 3-CA-degrading inoculant on reactor functions such as nitrification, carbon removal, and sludge compaction. Denaturing gradient gel electrophoresis (DGGE), FISH, and real-time PCR were used to examine the changes in the structure, abundance, and activity of the nitrifying community.

MATERIALS AND METHODS

SCAS reactors. The experiments were conducted with sludge freshly collected from a domestic wastewater treatment plant (Bourgoyen-Ossemeersen, Ghent, Belgium), by using a modified SCAS procedure (12). In brief, every 2 days, 200 ml of the mixed liquor was removed from the reactors (in 2-liter plastic Erlenmeyer flasks with an active volume of 1.2 liters) and 1.0 liter was allowed to settle for 30 min in an Imhoff cone, of which the upper 400 ml of the effluent was removed for analysis. The remaining settled sludge was poured back into the respective reactor, together with 600 ml of synthetic influent (skim milk powder [Gloria, Nestlé, Brussels, Belgium]; volumetric loading rate of 1 g of chemical oxygen demand [COD] liter^{-1} day^{-1}; COD/N/P ratio of 100:6:1) to bring the active reactor volume back to 1.2 liters. The SCAS reactors operated with a hydraulic retention time of 4 days and a sludge retention time of 12 days and contained 4 g of suspended solids liter^{-1}. To analyze sludge volume (SV), 1 liter of the mixed liquor was allowed to settle for 30 min in an Imhoff cone (24). The sludge volume index (SVI) was calculated by dividing the SV by the suspended solids (SS) (24).

All reactors were operated for 6 days before the experiment in order to allow the reactors to stabilize. On day 0, reactors 1 ($n = 2$) continued to receive only milk powder and were control reactors. In addition to the milk powder, reactors 2 ($n = 2$) and 3 ($n = 2$) both received on day 0 a shock load of 300 mg of 3-CA (Fluka AG Chemische Fabrik, Buchs, Switzerland; 99% pure), resulting in a final concentration of 250 mg liter^{-1} in the reactor mixed liquor. The bioaugmentation experiment was performed in reactors 3, in which *C. testosteroni* I2 *gfp* was inoculated. This strain, which has been chromosomally marked with *gfp* (the gene encoding green fluorescent protein), mineralizes 3-CA, fluoresces green under UV light and is rifampin (100 μg/ml) as well as kanamycin (50 μg/ml) resistant (12, 13). Luria broth (LB) agar supplemented with rifampin (100 mg liter^{-1}) and kanamycin (50 mg liter^{-1}) (both from Ducheva Haarlem, The Netherlands) was used to count I2 *gfp* (12).

The *C. testosteroni* I2 *gfp* inoculum was grown overnight at 28°C in 5 ml of LB medium (1 liter contains 5 g of NaCl, 10 g of tryptone, and 5 g of yeast extract) containing 100 mg of 3-CA liter^{-1}. Subsequently, 5-ml cultures were used to inoculate 200 ml of LB medium plus 3-CA (100 mg liter^{-1}). After overnight incubation at 28°C in a shaker (140 rpm; New Brunswick Scientific), the cultures were centrifuged (1 min at 5,000 × *g*), washed twice with saline (0.85% NaCl), and finally resuspended in saline. Reactors 3 were inoculated with *C. testosteroni* I2 *gfp* to a final concentration of $(5.4 \pm 0.37) \times 10^8$ cells/ml.

Sampling. Every 2 days, a sample was taken for high-performance liquid chromatography (HPLC) analysis, for DNA and RNA extraction, for FISH analysis, for plate counts of strain I2 *gfp*, and for determination of the SS and SVI (24). For DNA and RNA isolation, aliquots of the samples were immediately frozen at −20 and −80°C, respectively. For FISH, a subsample of activated sludge was fixed overnight with 4% paraformaldehyde (3).

Analytical methods. The effluent was analyzed for 3-CA content by reversed-phase HPLC after centrifugation at 5,000 × *g* for 10 min. The Summit HPLC system (Dionex, Wommelgem, Belgium) consisted of a Dionex pump series P580, a Dionex autosampler model ASI-100 (injection volume, 20 μl), an STH585 column oven (at 28°C), a Dionex UV/VIS UVD 340S detector, and Chromeleon software system version 6.10. A Hypersil Green Env column (150 by 8 mm [inner diameter]; 5-μm particle size [Alltech, Deerfield, Ill.]) was used. The mobile phase consisted of CH_3OH–0.1% H_3PO_4 (ratio, 70:30), with a flow rate of 0.8 ml/min. The UV detector was used at 210 nm.

The effluent was analyzed for nitrite, nitrate, and ammonium content by ion chromatography after centrifugation at 5,000 × *g* for 10 min and filtration through a 0.45-μm-pore-size filter. The DX-600 system (Dionex) consisted of a Dionex pump series GP50, a Dionex autosampler model AS50 (injection volume, 100 μl), a Dionex ED50 electrochemical detector, and PeakNet 6 software system version 6.10. Ionpac AS9-HC (250 by 4 mm [inner diameter]; 9-μm particle size [Dionex]) column and Ionpac CS12-HC (250 by 4 mm [inner diameter]; 8-μm particle size [Dionex]) were used for anion and cation separation, respectively. The mobile phase consisted of Na_2CO_3 (9 mM) and methanesulfonic acid (20 mM) for anion and cation analysis respectively, with a flow rate of 1 ml/min. The residual COD and SVI of the effluent were determined by standard methods (24).

DNA and RNA extraction from activated sludge. Total DNA extraction from the sludge samples and PCR conditions were based on the protocols described previously (12). The total RNA extraction protocol was adapted from those of Griffiths et al. (25) and Kowalchuk et al. (34). Briefly, in a 2-ml Eppendorf tube, 0.5 g of RNase-free 0.1-mm-diameter zirconia/silica beads (B. Braun Biotech International, Melsungen, Germany), 0.5 ml of activated sludge, 0.5 ml of CTAB buffer (5% [wt/vol] hexadecyltrimethylammonium bromide, 0.35 M NaCl, 120 mM potassium phosphate buffer [pH 8.0]), and 0.5 ml of phenol-chloroform-isoamyl alcohol mixture (25:24:1) were homogenized three times for 30 s each at 5,000 rpm in a Beadbeater (B. Braun Biotech International) with 10 s between shakings. Eppendorf tubes were spun centrifuged (5 min at 3,000 × *g*), and 300 μl of the supernatant was transferred to an RNase-free Eppendorf tube. Another 500 μl of CTAB buffer was added to the sludge suspension and homogenized again three times for 30 s each at 5,000 rpm in the Beadbeater with 10 s between shakings. Then 300 μl of the supernatant was added to the 300 μl taken from the first extraction, for a total of 600 μl. The phenol was removed by mixing with an equal volume of chloroform-isoamyl alcohol (24:1), inverting the tube, and centrifuging for 10 s. The upper, aqueous phase was transferred to a new Eppendorf tube, and nucleic acids were precipitated with 2 volumes of 30% (wt/vol) polyethylene glycol 6000–1.6 M NaCl for 2 h at room temperature. The Eppendorf tube was then centrifuged at 18,000 × *g* in a refrigerated centrifuge at 4 °C for 10 min. The nucleic acid pellet was subsequently washed in ice-cold 70% (vol/vol) ethanol and dried under vacuum for 10 min before being resuspended in 100 μL of RNase-free water. To obtain pure RNA a RQ1 RNase-Free DNase treatment was performed as specified by the manufacturer (Promega, Madison, Wis.). The average RNA yield was 3.4 ng ml of activated sludge^{-1}.

RT-PCR and PCR. The RNA was reverse transcribed to cDNA by using the Moloney murine leukemia virus (M-MLV) reverse transcriptase kit (Promega). Briefly, for each sample, 1 μl of each 10 mM deoxynucleoside triphosphate solution (Sigma-Aldrich Chemie, Steinheim, Germany), 1 μl of random hexamer primers (Sigma), 1 μl of extracted RNA, and 7 μl of DNase- and RNase-free filter-sterile water (Sigma) were mixed, incubated at 70°C for 10 min, and placed on ice. To each sample, a mixture was added containing 4 μl of 5× first-strand buffer (Promega), 2 μl of 0.1 M dithiothreitol (Promega), 1 μl of M-MLV reverse transcriptase (Promega), 0.5 μl of RNase inhibitor (Sigma), and 2.5 μl of DNase and RNase-free filter-sterile water (Sigma). The sample, containing a final vol-

Downloaded from http://aem.asm.org/ on October 23, 2019 by guest

TABLE 1. Sequences of the primers and probes used in this study

Primer or probe	Target	Sequence (5′ → 3′)	Reference
Primers			
P338F	*Bacteria*	ACTCCTACGGGAGGCAGCAG	49
P518r	Universal	ATTACCGCGGCTGCTGG	49
CTO189AB	β-*Proteobacteria* ammonia oxidizers	GGAGRAAAGCAGGGGATCG	34
CTO189C	β-*Proteobacteria* ammonia oxidizers	GGAGGAAAGTAGGGGATCG	34
CTO653r	β-*Proteobacteria* ammonia oxidizers	CTAGCYTTGTAGTTTCAAACG	34
GC-clamp		CGCCGGGGGCGCGCCCCGGGCGGGGCGGGGGCACGGGGGG	45
Probes			
NSO 190	β-*Proteobacteria* ammonia oxidizers	CGATCCCCTGCTTTTCTCC	44
EUB338	Most bacteria	GCTGCCTCCCGTAGGAGT	4
EUB338 II	*Planctomycetales*	GCAGCCACCCGTAGGTGT	18
EUB338 III	*Verrucomicrobiales*	GCTGCCACCCGTAGGTGT	18

ume of 20 μl, was incubated subsequently at 25°C for 10 min, 37°C for 3 h, and 94°C for 10 min. The cDNA was stored at 4°C (short-term storage) or −20°C (long-term storage).

A 1-μl volume of the DNA or cDNA was amplified as previously described (11). A list of the primers used in this study is given in Table 1. In brief, the 16S rRNA or rDNA for all members of the *Bacteria* were amplified by PCR using the forward primer P338F and the reverse primer P518r, and a GC-clamp of 40 bp was added to the forward primer. To amplify the 16S rDNA of the AOB, which belong to the β-*Proteobacteria*, a nested PCR approach was used. In the first PCR round, the forward primers were CTO189fAB and CTO189fC and the reverse primer was CTO653r, and in the second PCR round, primers P338F and P518r were used. After the first PCR round, a clearly visible band was present (the first PCR product was at least 0.3% of the total extracted DNA or cDNA), which suggested that no nonspecific amplification was expected in the second round (11). For more information about the specificity of the probes and primers listed in Table 1, see references 40 and 50.

DGGE analysis. DGGE based on the protocol of Muyzer et al. (45) was performed using the Bio-Rad D gene system (Bio-Rad, Hercules, Calif.). PCR fragments were loaded onto 8% (wt/vol) polyacrylamide gels in 1× TAE (20 mM Tris, 10 mM acetate, 0.5 mM EDTA [pH 7.4]). On each gel, a home-made marker of different PCR fragments was loaded, which was required for processing and comparing the different gels (11). The polyacrylamide gels were made with denaturing gradients ranging from 50 to 65% (12). The electrophoresis was run for 17 h at 60°C and 38 V. Staining and analysis of the gels were performed as described previously (12). Normalization and analysis of DGGE gel patterns were done with BioNumerics software version 2.0 (Applied Maths, Kortrijk, Belgium). During this processing, the different lanes are defined, background is subtracted, differences in the intensity of the lanes are compensated during normalization, and bands and band classes are detected. The band classes of the DGGE patterns were exported to EstimateS (15), a program which allows statistical analysis of species richness from samples by calculating the Chao2 index (16) using the equation $\text{Chao2} = S_{\text{obs}} + (L^2/2M)$, where S_{obs} is the observed number of species in a sample, L is the number of species that occur in only one sample ("unique species"), and M is the number of species that occur in exactly two samples. This is an incidence-based nonparametric estimator that uses presence absence data and can be used with 16S rRNA-DGGE patterns to obtain a first estimate of the community richness, making it a suitable index for PCR-based analysis (30, 54).

The calculation of the matrix of similarities is based on the Pearson product-moment correlation coefficient. The clustering algorithm of unpaired pair group method using arithmetic averages (UPGMA) was used to calculate dendrograms. Relevant and nonrelevant clusters were separated by the statistical cluster cutoff method (BioNumerics Manual 2.5).

Real-Time PCR. The real-time PCR was based on the principle of Heid et al. (27). For quantification of AOB by real-time PCR, amplification was performed in 25-μl reaction mixtures by using buffers supplied with the qPCR^T core kit for Sybr^T Green I as described by the suppliers (Eurogentec, Liège, Belgium) in MicroAmp Optical 96-well reaction plates with optical caps (PE Applied Biosystems, Nieuwerkerk a/d Ijssel, The Netherlands). Primers CTO189fAB, CTO189fC, and CTO653r and primers P338F and P518r (Table 1) were used for the quantification of AOB and the *Bacteria*, respectively, at a concentration of 300 nM. The PCR temperature program was as follows: 50°C for 2 min and 95°C for 5 min, followed by 40 cycles of 95°C for 15 s, 53°C (all *Bacteria*) or 57°C (AOB) for 30 s, and 60°C for 1 min. The template cDNA in the reaction mixtures was amplified ($n = 3$) and monitored with an ABI Prism SDS 7000 instrument (PE Applied Biosystems).

Standard curves constructed after real-time PCR amplification of five different DNA concentrations ($n = 4$) ranging from 5.0×10^5 to 5.0×10^3 copies of DNA/well were used. A 667-bp M13 PCR fragment of a *Nitrosomonas* sp. sequence (accession number AF525953) was generated as a template for the standard curve. The r^2 values were greater than 0.99 for both standard curves, and slopes of −3.87 and −3.68 were generated for AOB and all *Bacteria*, respectively. The relative number of rRNA molecules of the AOB was determined by dividing the number of AOB rRNA copies by the total number of bacterial rRNA molecules.

FISH. Sludge samples were fixed with fresh 4% paraformaldehyde solution, washed with phosphate-buffered saline, and stored in phosphate-buffered saline–ethanol (1:1) at −20°C until further processing (3). FISH assays were performed with fluorescently labeled, rRNA-targeted oligonucleotide probes by the method of Biesterfeld et al. (6). The following oligonucleotide probes were used (Table 1): (i) NSO190, specific for the AOB (labeled with sulfoindocyanine dye Cy3) and (ii) a mix of EUB338, EUB338-II, and EUB338-III, specific for the domain *Bacteria* (labeled with fluoresceine). Probes were obtained from Interactiva (Ulm, Germany).

Samples were analyzed by standard epifluorescence microscopy on an Axioskop II microscope (Carl Zeiss, Jena, Germany). The microscope was equipped with a Peltier cooled single-chip digital color charge-coupled device camera (Hamamatsu Orca IIIm, Hamamatsu, Massy Cedex, France) connected to a PC to obtain digital images. Quantification of cells was based on the procedure described by Daims et al. (19). In brief, TIFF files were exported by the image acquisition software and analyzed with MicroImage 4.0 (Media Cybernetics, Silver Spring, Md.). For each reactor from each day, five random pictures were recorded. The area fraction of stained AOB cells was calculated as a percentage of the total area of bacteria, stained with the EUB338 probe mix.

DNA sequencing. 16S rDNA gene fragments were cut out of the DGGE gel with a clean scalpel and added to 50 μl of PCR water. After 12 h of incubation at 4°C, 1 μl of the PCR water was reamplified with primer set P338F and P518r. Then 5 μl of the PCR product was loaded onto a DGGE gel (see above), and if the DGGE pattern showed only one band, it was sent out for sequencing. DNA sequencing of the ca. 180-bp fragments was carried out by ITT Biotech-Bioservice (Bielefeld, Germany). Analysis of DNA sequences and homology searches were completed with standard DNA sequencing programs and the BLAST server of the National Center for Biotechnology Information (NCBI) using the BLAST algorithm (2).

Nucleotide sequence accession numbers. Nucleotide sequences for bands 1 through 5 have been deposited in the GenBank database under accession numbers AF479281 to AF479285.

Downloaded from http://aem.asm.org/ on October 23, 2019 by guest

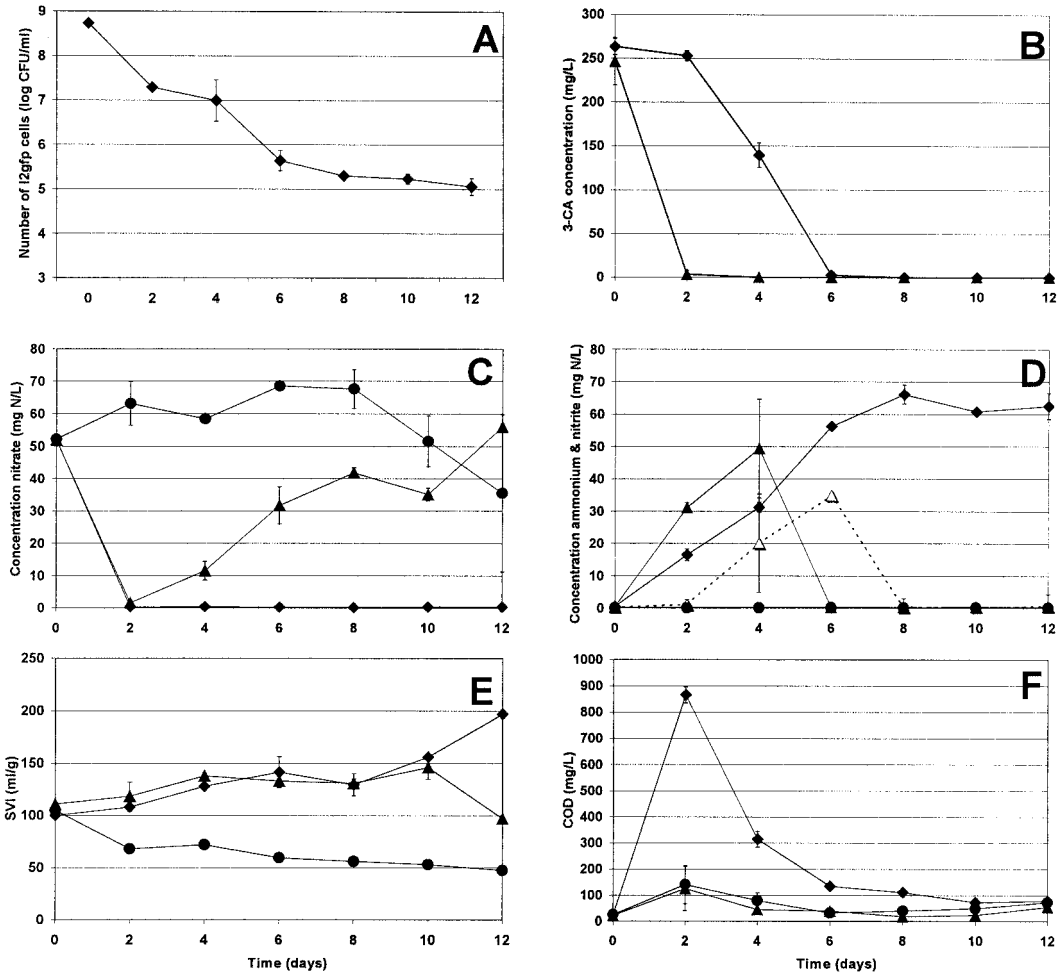

FIG. 1. Data obtained from the different types of reactors. Reactors 1 were not bioaugmented, and no 3-CA shock was applied (●); reactors 2 were not bioaugmented but were exposed to a 3-CA shock load (◆); reactors 3 were bioaugmented and exposed to a 3-CA shock load (▲). (A) Survival of *C. testosteroni* I2 *gfp* cells in reactors 3; (B) concentration of 3-CA in reactors 2 and 3 in the effluent; (C) nitrate concentration in the effluent; (D) ammonium (solid symbols, solid line) and nitrite (open symbols, dotted line) concentrations in the effluent; (E) settlement of the activated sludge, expressed as SVI; (F) COD concentration in the effluent. Values represent the mean and standard error of results from two reactors ($n = 2$); in some cases, the error bars were too small to illustrate.

RESULTS

SCAS reactor performance. Three different pairs of reactors were examined. The first pair of reactors was used as a control, with no inoculation or shock load applied (reactors 1). The second pair consisted of the 3-CA-treated reactors (disturbed reactors); they received a shock load treatment of 3-CA on day 0 (reactors 2). The third pair of reactors were the bioaugmented reactors, which received the same 3-CA pulse on day 0 but were also inoculated with *C. testosteroni* I2 *gfp* cells (reactors 3). The number of I2 *gfp* cells decreased ca. 3 log units after inoculation and stabilized after 6 days at 10^5 CFU ml^{-1} (Fig. 1A). As a result of the inoculation in reactors 3, the I2 *gfp* cells had removed all detectable 3-CA 48 h after inoculation (Fig. 1B). In reactors 2 without I2 *gfp*, 3-CA persisted until day 6, and its removal was due solely to washout (the hydraulic retention time of the system was 4 days) and not to (bio)degradation.

The 3-CA shock inhibited nitrification for an extended period despite its disappearance by day 2 in the protected reactors and day 6 in the nonbioaugmented reactors (Fig. 1C and D). In nonbioaugmented reactors 2, nitrite and nitrate concentration remained very low and ammonium accumulated for the duration of the experiment. From day 4, nitrification in the bioaugmented reactors 3 recovered, resulting in the accumulation of nitrate (Fig. 1C) and nitrite (Fig. 1D). The nitrite was present in reactors 3 until day 6, but by day 8, all the nitrite was removed. The restored nitrification activity resulted in the complete removal of ammonium from day 6 (Fig. 1D). In both reactors that received the 3-CA pulse, the SVI increased, indicating that the settlement of the activated sludge was poor (Fig. 1E). In contrast to nitrification, the SVI did not recover in the bioaugmented reactors during the first 10 days; however, the sludge compactability improved on day 12. Only the nonbioaugmented shock-loaded reactors 2 accumulated large amounts of COD (Fig. 1F). However, from day 4, COD removal increased again. The bioprotection of reactors 3 was

Downloaded from http://aem.asm.org/ on October 23, 2019 by guest

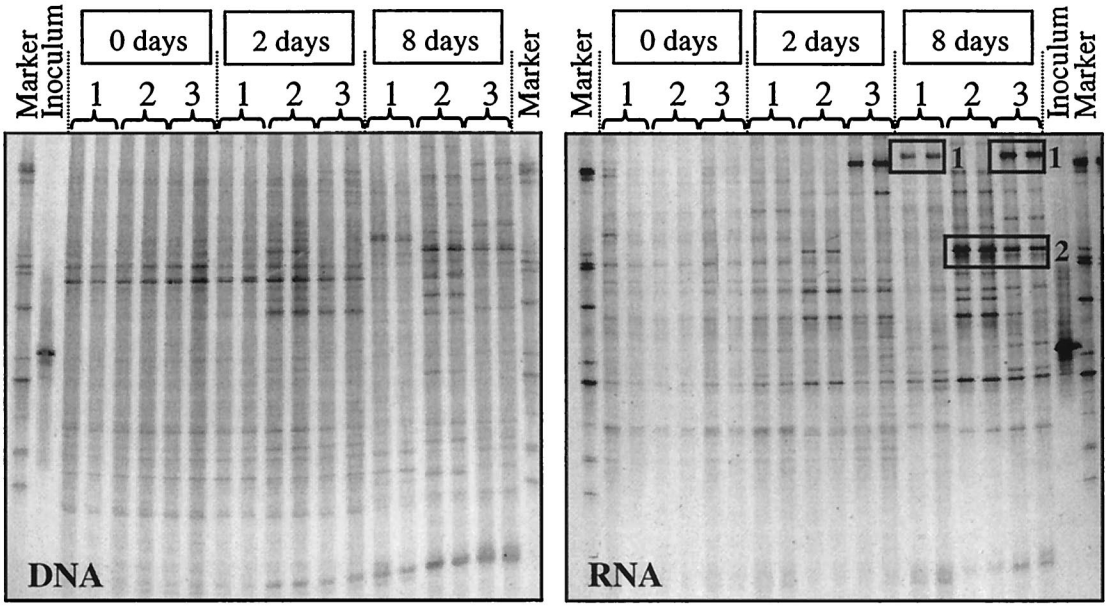

FIG. 2. Analysis of the DGGE profiles of the different reactors on days 0, 2, and 8, using partial bacterial 16S rRNA gene fragments (bp 338 to 518), based on extracted DNA and RNA. Boxed areas indicate the bands excised and sequenced for further analysis; the accession numbers of the most similar sequences in GenBank are mentioned in the text. Lanes: 1, reactors without inoculant and without 3-CA shock; 2, nonbioaugmented reactors with 3-CA shock load; 3, bioaugmented reactors with 3-CA shock load

very effective, and no differences in COD removal compared to control reactors 1 were observed.

DGGE analysis of the *Bacteria*. To relate the observed changes in function to changes in the community structure and diversity, 16S rDNA and 16S rRNA DGGE analyses were performed with bacterial primers. Since days 0, 2, and 8 were considered to be typical for the microbial community, with day 0 representing the community just before disruption, day 2 representing disruption (inhibition of certain functions), and day 8 representing recovery, these samples were analyzed by DGGE in detail. Visual comparison of the RNA DGGE patterns at day 8 allowed us to select two bands that were clearly different among the differently treated reactors. On day 8, in nondisturbed reactors 1 and bioaugmented reactors 3, there was a prominent band in the RNA DGGE gel (Fig. 2, band 1), with a sequence having low similarity to members of the *Cytophaga-Flavobacter* group (146 of 168 bp with the uncultured bacterial clone AF369713.1, and 98 of 104 bp with *Cytophaga* sp. strain AJ224415.1 [39], a fragment isolated from a nitrifying reactor system). This band was not visible in the patterns of the 3-CA-treated reactors, which could indicate that the corresponding organism was very sensitive to the toxic shock. Another fragment, band 2, present only in reactors receiving 3-CA (reactors 2 and 3), is identical to the sequence of the gram-positive actinomycete *Nostocoida limicola* AF255736.1 (177 of 177 bp; sequence isolated from a bulking filamentous bacterium in a reactor treating industrial waste). The clear presence of this band in the fingerprint might be an indication that this corresponding organism is more resistant to the 3-CA shock load.

The differences between the DGGE patterns based on extracted RNA and DNA were evaluated by cluster analysis and calculation of the Chao2 richness estimator. The RNA-based DGGE patterns for all bacteria contained fewer bands than the DNA-based DGGE patterns (Fig. 2). This observation was confirmed by the Chao2 richness estimator, obtained by numerical analysis of the DGGE patterns: the values obtained for the DNA DGGE patterns were always higher than for the RNA DGGE profiles (data not shown). This indicates that not all the microorganisms present were highly active. However, it is also possible that the RNA DGGE analysis was confounded by one or a few strains that produce large amounts of rRNA and thus the RNA concentrations of several other active species may have fallen below the presumed 1% detection limit, typical for PCR-DGGE (45).

On day 0, several faint bands and just one or two dominant ribotypes were present in both DGGE patterns. The DGGE patterns for the DNA and the RNA samples were very reproducible, since only small differences between the patterns from day 0 and from the duplicate reactors were noticeable. Cluster analysis confirmed these observations (Fig. 3). During the experiment, certain bands became more dominant while some faint bands became invisible. As a result, fewer bands were detected from day 2 and the Chao 2 richness decreased during the experiment in all reactors compared with day 0 (data not shown). Cluster analysis of the DNA DGGE patterns showed that the reactors on days 0 and 2 formed one large cluster while each reactor on day 8 produced a distinctive group. Cluster analysis of the RNA DGGE revealed three clusters. The samples from day 0 and the control reactors 1 from day 2 formed one cluster. From day 2, the observed changes in the microbial community structure of reactors 2 were different from those of the other reactors. A third cluster consisted of reactors 3 from days 2 and 8 and of reactors 1 from day 8.

DGGE analysis of AOB. Since the 3-CA shock and the bioprotection had a major influence on the nitrification activity

Downloaded from http://aem.asm.org/ on October 23, 2019 by guest

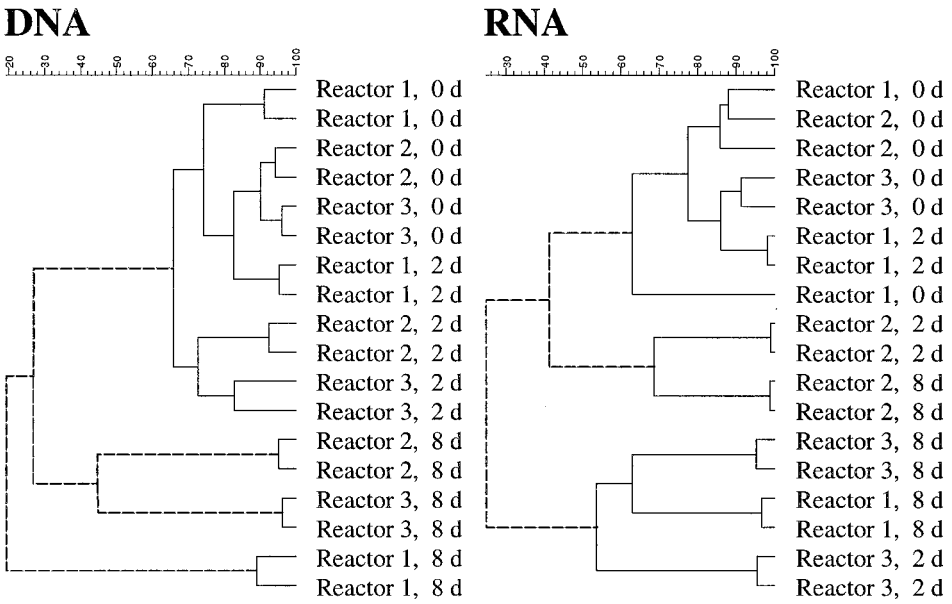

FIG. 3. Cluster analysis of the bacterial DGGE patterns based on DNA and RNA samples from the different reactors 1, 2, and 3 (Fig. 2). The dendrogram was calculated on the basis of the Pearson product-moment correlation coefficient with the UPGMA clustering algorithm. Significant (solid lines) and nonsignificant (dotted lines) clusters were separated by the statistical cluster cutoff method. d, days.

in reactors 2 and 3, a more detailed analysis of the AOB was performed. On day 0 (good nitrification activity before the shock), DGGE patterns obtained with primers for AOB were very similar, even between the RNA and DNA samples (Fig. 4). A visual comparison of the RNA DGGE patterns showed that two bands seemed to play a critical role in the nitrification (bands 3 and 4). These two intense bands were excised from the RNA DGGE gel and sequenced (Fig. 4). The upper band, band 3, showed highest similarity to an uncultured *Nitrosomonas* strain AJ245752.1 (173 of 173 bp; sequence obtained from a selective enrichment of AOB from a sediment) and to an uncultured member of the β-*Proteobacteria*, AJ299051.1 (177 of 177 bp [9]; sequence of an AOB enriched from a freshwater sediment), while the lower band, band 4, matched with a *Ni-*

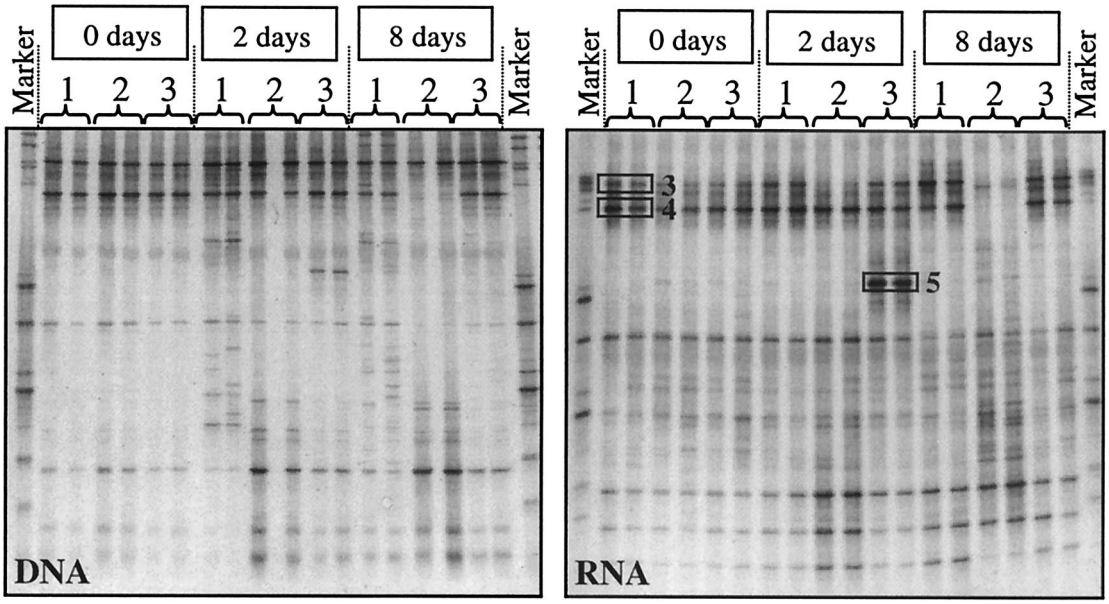

FIG. 4. Analysis of the DGGE profiles of the different reactors on days 0, 2, and 8, using partial bacterial 16S rRNA gene fragments, based on DNA and RNA. The gene fragments were obtained by using an AOB-specific PCR with primers CTO189AB, CTO189C, and CTO653r (Table 1), followed by a second PCR with bacterial primers P338F and P518r (Table 1). Bands 3, 4, and 5 were excised and sequenced for further analysis. Lanes: 1, reactors without inoculant and without 3-CA shock; 2, nonbioaugmented reactors with 3-CA shock load; 3, bioaugmented reactors with 3-CA shock load. The accession numbers of the most similar sequences in GenBank are mentioned in the text.

Downloaded from http://aem.asm.org/ on October 23, 2019 by guest

trosococcus/Nitrosomonas strain (174 of 177 bp were identical to the corresponding sequence of *Nitrosococcus mobilis* AF287297.1 [50], AJ298728.1 [1], and M96403.1 [26] and *Nitrosomonas* sp. strain AF272415.1 [50]). In the lower part of the DGGE gels, a few other bands were present as well, but no effect of the treatments on the corresponding populations were observed. Although nitrification was inhibited in reactors 2 as well as reactors 3, 2 days after the shock load, the RNA DGGE patterns of the AOB community structure differed between these two reactors. On day 2 in reactor 2, band 3 was hardly visible in the RNA DGGE patterns, and after 8 days, both bands 3 and 4 had almost disappeared. In the bioaugmented reactors 3, however, both bands 3 and 4 were still clearly detectable on day 2. Interestingly, a third potential AOB, represented by band 5, identified as an uncultured member of the β-*Proteobacteria*, became more dominant. The DNA sequence of this fragment was identical (171 of 172 bp) to a sequence submitted to GenBank (AJ245760.1, obtained by selective enrichment of ammonia-oxidizing bacteria in freshwater sediments). This DNA fragment was obtained by this group by using the same specific primers for AOB that were used in our study (H. J. Laanbroek, personal communication). The first known sequence of an AOB similar to band 5 is *N. mobilis* (155 of 176 bp identical, or 88% similarity; accession number AF287297.1 [50]). By day 8, when nitrification was restored in the bioaugmented reactors 3, the RNA DGGE profiles were similar to their original pattern and the additional band 5 had disappeared.

Quantification of the AOB by FISH and real-time PCR. The DGGE analysis showed that shifts occurred in the AOB community. Since it is not possible to obtain quantitative data from the DGGE patterns, real-time PCR and FISH were used to examine the prevalence of the AOB in the activated sludge. On days 0, 2, and 8, the number of rRNA molecules present in the reactors was estimated by amplifying the 16S rRNA cDNA of the *Bacteria* and the AOB from the different reactors and measuring the increasing amounts of amplification products. The relative number of AOB was estimated by dividing the number of AOB rRNA copies by the total number of bacterial rRNA copies (Fig. 5). The data showed that the relative number of rRNA copies of the AOB decreased after 2 days, both in the bioaugmented and in the nonbioaugmented reactors. At 8 days after the shock load, the number of rRNA copies of the AOB decreased further in the nonbioaugmented reactors, while in the bioprotected reactors the number had increased again. To confirm the trend observed in the real-time PCR data, FISH analysis was also applied. From the different reactors on days 0 and 8, the area of all the bacteria and of the AOB was measured and the ratio of AOB and bacteria was calculated. On day 0, clusters of AOB could be observed in the activated sludge flocs and an area-based calculation estimated that 2.23% ± 0.76% of the area consisted of AOB. By day 8, AOB clusters were detected only in the reactors where nitrification was observed, i.e., reactors 1 (1.73% ± 0.76%) and 3 (1.60% ± 0.05%), whereas in reactor 2, almost no AOB flocs were observed (0.47% ± 0.59%). The results of the real-time PCR and the FISH quantification indicate that the number of 16S rRNA molecules of the AOB decreased drastically in reactor 2 from day 0 to day 8, while the populations seemed largely protected by bioaugmentation with the 3-CA degrading strain. This confirms the interpretation formulated above based on the RNA DGGE patterns, i.e., that the nitrifying community had recovered from the 3-CA pulse in the bioaugmented reactors only.

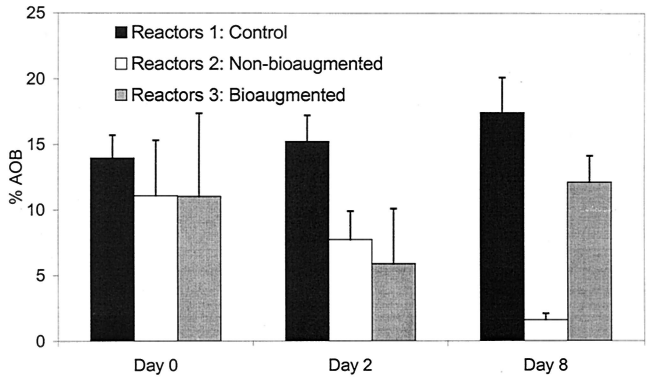

FIG. 5. Relative abundance of cDNA of AOB in activated-sludge reactors, as determined by real-time PCR. Values represent the mean and standard error ($n = 3$).

Microscopic analysis of cell and floc morphologies. To explain the altered settlement characteristics of reactors 2 and 3, the floc structures in the different reactors were examined by light microscopy (data not shown). On day 0, a limited number of filaments were present. In the control reactors 1, the sludge floc structure did not change after 8 days and the number of filaments did not increase. However, in the shock-loaded reactors 2 and 3, where an increased SVI was observed, the number of filaments was larger on day 8 than on day 0.

DISCUSSION

We investigated the effects of 3-CA shock load on the basic functions of a wastewater treatment reactor and focused on the recovery of major functional activities. Moreover, bioaugmentation by the inoculation of a 3-CA-degrading strain was used to investigate whether rapid 3-CA removal could decrease the recovery period. The most drastic effect of the 3-CA shock load observed was on the nitrification activity. Initially, nitrification was totally inhibited in reactors 2 and 3 where a 3-CA shock load was applied. The nonsubstituted form of 3-CA, aniline, is known to inhibit nitrification (22, 23), and, like most inhibitors, aniline inhibits nitrification activity by acting as a suicide substrate for ammonium monooxygenase (43). It is likely that 3-CA inhibition is based on the same mechanism (D. J. Arp, personal communication). As a consequence, reestablishment of the nitrification activity in the activated sludge after the removal of the inhibitor through degradation or washout requires de novo synthesis of the enzymes. After 2 days in the bioaugmented reactors 3, 3-CA was degraded completely, allowing the slow recovery of nitrification activity, which was visible from day 4 (Fig. 1). The observed temporal accumulation of nitrite is normal during the startup period of nitrification (36, 57).

In the RNA DGGE profiles of the AOB community, an additional very intense band appeared on day 2 in the bioaugmented reactors 3. In the corresponding DNA DGGE patterns of day 2, the species corresponding to this extra band was

Downloaded from http://aem.asm.org/ on October 23, 2019 by guest

represented by a weak band but did not appear to be the most numerically dominant. These data, taken together, suggest that this bacterial population represented by band 5 became a relatively more abundant and highly active member of the community. This population may have had a selective advantage over the other two populations, represented by bands 3 and 4. Work by Suwa et al. (53) showed that various *Nitrosomonas* strains isolated from activated sludge could be either sensitive or insensitive to ammonium. The short-term inhibition of nitrification by 3-CA led to an accumulation of ammonium, which may have inhibited the organisms represented by bands 3 and 4. Band 5, which may represent an AOB that is insensitive to higher ammonium concentrations, would then be able to become more dominant and more active. Thus, as the rRNA content of the two initial dominating AOB (bands 3 and 4) decreased relative to band 5, the new band became visible as a large fraction of the total RNA (band 5). From day 4, the ammonium concentration decreased again, such that the nitrification activity by the original AOB (bands 3 and 4) was restored while the other population (band 5) appeared to be outcompeted again. In the nonbioaugmented reactor 2, band 5 was never visible since the corresponding organism was probably also inhibited by the high 3-CA concentration. In these reactors 2, the 3-CA was present for 4 days, in contrast to less than 2 days in the bioaugmented reactors 3 (Fig. 1B), and thus the entire nitrifying community was apparently inhibited during this time. Although 3-CA levels were undetectable by day 6, no nitrification recovery was observed in reactors 2. A contact time of 4 days with 3-CA seemed to be critical for the AOB. This was corroborated by the disappearance of the two dominant bacteria of the AOB community on day 8, as indicated in the RNA DGGE patterns for reactors 2. The results of real-time PCR and FISH analysis confirmed the negative effect of the 3-CA exposure on the community of AOB, since hardly any AOB cells or clusters could be detected in reactors 2 on day 8. Nitrification would possibly recover in the nonbioaugmented reactors if the experiment were prolonged, allowing the AOB to proliferate again.

The higher SVI in reactors 2 and 3 was clearly a result of the 3-CA shock load. Microscopy revealed a larger number of filaments in both reactors, and sequencing of a dominant band in the RNA DGGE profiles of reactors 2 and 3 revealed the presence of an actinomycete (AF255736.1), i.e., *Nostocoida limicola.* This species has been related to the decline of sludge settling properties in a large number of studies (37, 60), and an increased number of filaments has been shown to correspond to higher SVI values (37, 41, 47). It is well known that actinomycetes exhibit the capacity to metabolize recalcitrant molecules (42). The actinomycete-like filaments in the shock-loaded reactors 2 and 3 may be the result of improved resistance to 3-CA.

After the 3-CA shock, a higher COD concentration in the effluent of the nonbioaugmented reactors 2 was observed. The heterogeneous nature of wastewaters allows the development of diverse heterotrophic bacterial populations. From day 4, the COD removal was essentially restored; the higher COD concentrations in these reactors on day 4 were presumably due to the residual 3-CA concentration (ca. 150 of the extra 200 mg/liter), which was gradually washed out. The effect of inoculation of *C. testosteroni* I2 *gfp* into the shock-loaded reactors was striking: COD removal capacity was not lowered, resulting in a full protection of the activated sludge and COD levels comparable to the non-shocked control reactors 1. There are different factors that can explain the increased COD concentrations in the effluent of the nonbioaugmented reactors 2: (i) the indigenous bacteria, responsible for the COD removal, could be temporarily inhibited by the long 3-CA shock; (ii) the protozoa, important predators of bacteria, could be inhibited, resulting in an increased number of dispersed bacteria in the effluent; or (iii) the toxicity of the 3-CA could have resulted in the lysis of a part of the biomass. Some combination of all these factors is also a possible explanation for the increased COD on day 2 in reactors 2.

Methods based on direct PCR amplification and analysis of rRNA genes by DGGE or temperature gradient gel electrophoresis (TGGE) are frequently used to examine the microbial community structure and microbial diversity of environmental samples (17, 20, 46, 56). However, PCR-based techniques can be biased (54). The number and intensity of bands in a DGGE pattern do not necessarily give an accurate picture of the microbial community. Because of the shortcomings inherent to DGGE based on PCR-amplified rRNA gene sequences, the estimators calculated from the DGGE banding patterns must be interpreted as only an indication and not an absolute measure of the degree of diversity in a bacterial community (20). Also, one organism may produce more than one DGGE band because of multiple, heterogeneous rRNA operons (14, 48, 51) and one DGGE band may represent several species with identical partial 16S rDNA sequences (55). In a mixture of target rRNA genes present at very different concentrations, the less abundant sequences are not amplified sufficiently to be visualized as bands on a DGGE gel, and therefore, the banding pattern reflects only the most abundant rRNA types in the microbial community (45). This is why the inoculated strain could hardly be seen in the DGGE patterns on day 2 in the bioaugmented reactors 3. On day 8, the inoculated strain was not detectable any more, most probably because its proportion of the total bacterial cell numbers had become too small. In our previous work, the same inoculum was also not visible in the DGGE patterns of bioaugmented activated sludge (12). Another bias is the shortcoming of primers and probes concerning their specificity. The work of Purkhold et al. (50) clearly demonstrated that at the moment, there is no perfect primer or probe set to study AOB. The CTO primer set used in this study also matches with some non-AOB strains (50), and therefore it cannot be excluded that some of the bands in the DGGE patterns may be not related to AOB.

In this study, we used DGGE analysis based on extracted DNA as well as RNA to evaluate changes in the sludge microbial communities. It appears from the bacterial DGGE patterns that the number of numerically dominant populations present was larger than the number of abundant and highly active populations: on day 0, the bacterial richness based on the RNA DGGE patterns was markedly lower than for the DNA DGGE patterns. This suggests a lower bacterial richness among the active numerically dominant populations than among the total (dead, dormant, and active) dominant populations. Some very active populations, visible in the RNA DGGE patterns, can hardly be detected in the DNA DGGE fingerprints. This shows that DNA-based analyses do not al-

Downloaded from http://aem.asm.org/ on October 23, 2019 by guest

ways reflect the most active members of the microbial community. DNA obtained form environmental samples could originate from dormant or dead cells (32) or even from free DNA. This is also reflected in the analysis of the AOB: based on the DNA DGGE, only some small differences in the minor bands were visible on days 0 and 2, while the RNA DGGE clearly showed differences in the dominant bands, as discussed above. This difference may reflect differences in the activity of the nitrifying species between these two time points. A similar phenomenon was observed for RNA TGGE fingerprints of grassland soil bacterial communities, which were less diverse than the DNA TGGE fingerprints (21). Numerical analysis of our DGGE results also indicated that the significant clusters of the RNA DGGE patterns reflect better the metabolic state of the different reactors than the DNA DGGE patterns do. The DNA DGGE cluster analysis showed one large cluster of days 0 and 2, while after 8 days every set of duplicate reactor formed a separate cluster. In contrast, the RNA DGGE analysis resulted in three distinct clusters: (i) all reactors before day 0 and control reactors 1 on day 2, (ii) the shock-loaded and disturbed reactors 2 on days 2 and 8 and (iii) the control reactors 1 on day 8 and the bioaugmented-recovered reactors 3 on days 2 and 8. Therefore, RNA DGGE analysis is appropriate to examine rapidly changing microbial communities while DNA DGGE analysis appears sufficient for slowly evolving, stable communities.

This study has demonstrated that a 3-CA shock load disrupted the basic metabolic functions of activated sludge. Inoculation with a bacterial strain capable of 3-CA mineralization protected the performance of the reactors and allowed a rapid recovery of nitrification. Some of these functional changes were explained by changes in the structure of the overall bacterial community, specifically of the AOB community. Although evaluation of the eventual success of this bioaugmentation strategy at field scale requires further experiments, in particular under conditions of post-shock inoculations, our work clearly indicates that inoculation of wastewater treatment systems subject to toxic shock loads, with a specific degrader of the toxic compound, can result in faster recovery of essential metabolic functions.

ACKNOWLEDGMENTS

This work was supported by project grant G.O.A. (1997-2002) of the "Ministerie van de Vlaamse Gemeenschap, Bestuur Wetenschappelijk Onderzoek" (Belgium) and by an equipment grant (epifluorescence microscope) of the Flemish Fund for Scientific Research (FWO-Vlaanderen)

We thank Daniel J. Arp for useful suggestions; Frederik Hammes for microscopic evaluation; Katrien Crul, Siska Maertens, and Leen De Gelder for their assistance during the molecular work; and Wim De Windt, Dave Seghers, Thomas Vande Sijpe, and Kristof Verthé for critically reading the manuscript.

REFERENCES

1. **Aakra, A., J. B. Utaker, A. Pommerening-Roser, H. P. Koops, and I. F. Nes.** 2001. Detailed phylogeny of ammonia-oxidizing bacteria determined by rDNA sequences and DNA homology values. Int. J. Syst. Evol. Microbiol. **51:**2021–2030.
2. **Altschul, S. F., T. L. Madden, A. A. Schaffer, J. Zhang, Z. Zhang, W. Miller, and D. J. Lipman.** 1997. Gapped BLAST and PSI-BLAST: a new generation of protein database search programs. Nucleic Acids Res. **25:**3389–3402.
3. **Amann, R. I.** 1995. In situ identification of micro-organisms by whole cell hybridization with rRNA-targeted nucleic acid probes, p. 1–15. *In* A. D. L. Akkermans, J. D. van Elsas, and F. J. de Bruijn (ed.), Molecular microbial ecology manual. Kluwer Academic Publishers, Dordrecht, The Netherlands.
4. **Amann, R. I., B. J. Binder, R. J. Olson, S. W. Chisholm, R. Devereux, and D. A. Stahl.** 1990. Combination of 16S rRNA-targeted oligonucleotide probes with flow cytometry for analyzing mixed microbial populations. Appl. Environ. Microbiol. **56:**1919–1925.
5. **Amann, R. I., W. Ludwig, and K. H. Schleifer.** 1995. Phylogenetic identification and in situ detection of individual microbial cells without cultivation. Microbiol. Rev. **59:**143–169.
6. **Biesterfeld, S., L. Figueroa, M. Hernandez, and P. Russell.** 2001. Quantification of nitrifying bacterial populations in a full-scale trickling filter using fluorescent *in situ* hybridisation. Water Environ. Res. **73:**329–338.
7. **Bitton, G.** 1994. Toxicity testing in wastewater treatment plants using microorganisms: wastewater microbiology. Wiley-Liss, New York, N.Y.
8. **Blackall, L. L., P. C. Burrell, H. Gwilliam, D. Bradford, P. L. Bond, and P. Hugenholtz.** 1998. The use of 16S rDNA clone libraries to describe the microbial diversity of activated sludge communities. Water Sci. Technol. **37:**451–454.
9. **Bollmann, A., and H. J. Laanbroek.** 2001. Continuous culture of ammonia-oxidising bacteria at low ammonium concentrations. FEMS Microbiol. Ecol. **37:**211–221.
10. **Boon, N., L. De Gelder, H. Lievens, S. D. Siciliano, E. M. Top, and W. Verstraete.** 2002. Bioaugmenting bioreactors for the continuous removal of 3-chloroaniline by a slow release approach. Environ. Sci. Technol. **36:**4698–4704.
11. **Boon, N., W. De Windt, W. Verstraete, and E. M. Top.** 2002. Evaluation of nested PCR-DGGE (denaturing gradient gel electrophoresis) with group-specific 16S rRNA primers for the analysis of bacterial communities from different wastewater treatment plants. FEMS Microbiol. Ecol. **39:**101–112.
12. **Boon, N., J. Goris, P. De Vos, W. Verstraete, and E. M. Top.** 2000. Bioaugmentation of activated sludge by an indigenous 3-chloroaniline degrading *Comamonas testosteroni* strain, I2 *gfp.* Appl. Environ. Microbiol. **66:**2906–2913.
13. **Boon, N., J. Goris, P. De Vos, W. Verstraete, and E. M. Top.** 2001. Genetic diversity among 3-chloroaniline and aniline degrading strains of the *Comamonadaceae.* Appl. Environ. Microbiol. **67:**1107–1115.
14. **Cilia, V., B. Lafay, and R. Christen.** 1996. Sequence heterogeneities among 16S ribosomal RNA sequences, and their effect on phylogenetic analyses at the species level. Mol. Biol. Evol. **13:**451–461.
15. **Colwell, R. K.** 1997. EstimateS: statistical estimation of species richness and shared species from samples, version 5. User's Guide and application published at http://viceroy.eeb.uconn.edu/estimates.
16. **Colwell, R. K., and J. A. Coddington.** 1994. Estimating terrestrial biodiversity through extrapolation. Philos. Trans. R. Soc. London Ser. B **345:**101–118.
17. **Curtis, T. P., and N. G. Craine.** 1998. The comparison of the diversity of activated sludge plants. Water Sci. Technol. **37:**71–78.
18. **Daims, H., A. Bruhl, R. Amann, K. H. Schleifer, and M. Wagner.** 1999. The domain-specific probe EUB338 is insufficient for the detection of all *Bacteria*: development and evaluation of a more comprehensive probe set. Syst. Appl. Microbiol. **22:**434–444.
19. **Daims, H., N. B. Ramsing, K. H. Schleifer, and M. Wagner.** 2001. Cultivation-independent, semiautomatic determination of absolute bacterial cell numbers in environmental samples by fluorescence in situ hybridization. Appl. Environ. Microbiol. **67:**5810–5818.
20. **Eichner, C. A., R. W. Erb, K. N. Timmis, and I. Wagner-Döbler.** 1999. Thermal gradient gel electrophoresis analysis of bioprotection from pollutant shocks in the activated sludge microbial community. Appl. Environ. Microbiol. **65:**102–109.
21. **Felske, A., and A. D. L. Akkermans.** 1998. Spatial homogeneity of abundant bacterial 16 S rRNA Molecules in Grassland soils. Microb. Ecol. **36:**31–36.
22. **Ficara, E., and A. Rozzi.** 2001. pH-stat titration to assess nitrification inhibition. J. Environ. Eng. **127:**698–704.
23. **Gheewala, S. H., and A. P. Annachhatre.** 1997. Biodegradation of aniline. Water Sci. Technol. **36:**53–63.
24. **Greenberg, A. E., L. S. Clesceri, and A. D. Eaton** (ed.). 1992. Standard methods for the examination of water and wastewater, 18th ed. American Public Health Association, American Water Works Association, and Water Environment Federation, Washington D.C.
25. **Griffiths, R. I., A. S. Whiteley, A. G. O'Donnell, and M. J. Bailey.** 2000. Rapid method for coextraction of DNA and RNA from natural environments for analysis of ribosomal DNA- and rRNA-based microbial community composition. Appl. Environ. Microbiol. **66:**5488–5491.
26. **Head, I. M., W. D. Hiorns, T. M. Embley, A. J. McCarthy, and J. R. Saunders.** 1993. The phylogeny of autotrophic ammonia-oxidising bacteria as determined by analysis of 16S ribosomal RNA gene sequences. J. Gen. Microbiol. **139:**1147–1153.
27. **Heid, C., J. Stevens, K. Livak, and P. Williams.** 1996. Real time quantitative PCR. Genome Res. **6:**986–994.
28. **Henckel, T., M. Friedrich, and R. Conrad.** 1999. Molecular analyses of the methane-oxidizing microbial community in rice field soil by targeting the genes of the 16S rRNA, particulate methane monooxygenase, and methanol dehydrogenase. Appl. Environ. Microbiol. **65:**1980–1990.
29. **Henze, M.** 1990. Basic biological processes, p. 83–85. *In* M. Henze, P. Har-

Downloaded from http://aem.asm.org/ on October 23, 2019 by guest

remoës, and E. Arvin (ed.), Wastewater treatment. Springer-Verlag KG, Heidelberg, Germany.
30. **Hughes, B. J., J. J. Hellmann, T. H. Ricketts, and B. J. M. Bohannan.** 2001. Counting the uncountable: statistical approaches to estimating microbial diversity. Appl. Environ. Microbiol. **67:**4399–4406.
31. **Iwamoto, T., K. Tani, K. Nakamura, Y. Suzuki, M. Kitagawa, M. Eguchi, and M. Nasu.** 2000. Monitoring impact of *in situ* biostimulation treatment on groundwater bacterial community by DGGE. FEMS Microbiol. Ecol. **32:** 129–141.
32. **Josephson, K. L., C. P. Gerba, and T. L. Pepper.** 1993. Polymerase chain reaction of nonviable bacterial pathogens. Appl. Environ. Microbiol. **59:** 3513–3515.
33. **Kearney, P. C., and D. D. Kaufman.** 1969. Degradation of herbicides. Marcel Dekker, Inc., New York, N.Y.
34. **Kowalchuk, G. A., P. L. E. Bodelier, G. H. J. Heilig, J. R. Stephen, and H. J. Laanbroek.** 1998. Community analysis of ammonia-oxidising bacteria, in relation to oxygen availability in soils and root-oxygenated sediments, using PCR, DGGE and oligonucleotide probe hybridisation. FEMS Microbiol. Ecol. **27:**339–350.
35. **Kowalchuk, G. A., and J. R. Stephen.** 2001. Ammonia-oxidising bacteria: a model for molecular microbial ecology. Annu. Rev. Microbiol. **55:**485–529.
36. **Lekang, O.-I., and H. Kleppe.** 2000. Efficiency of nitrification in trickling filters using different filter media. Aquacult. Eng. **21:**181–199.
37. **Lemmer, H., G. Lind, E. Muller, M. Schade, and B. Ziegelmayer.** 2000. Scum in activated sludge plants: Impact of non-filamentous and filamentous bacteria. Acta Hydrochim. Hydrobiol. **28:**34–40.
38. **Liu, W. T., T. L. Marsh, and L. J. Forney.** 1998. Determination of the microbial diversity of anaerobic-aerobic activated sludge by a novel molecular biological technique. Water Sci. Technol. **37:**417–422.
39. **Logemann, S., J. Schantl, S. Bijvank, M. van Loosdrecht, J. G. Kuenen, and M. S. M. Jetten.** 1998. Molecular microbial diversity in a nitrifying reactor system without sludge retention. FEMS Microbiol. Ecol. **27:**239–249.
40. **Loy, A., M. Horn, and M. Wagner.** 2003. ProbeBase—an online resource for rRNA-targeted oligonucleotide probes. Nucleic Acids Res. **31:**514–516.
41. **Madoni, P., D. Davoli, and G. Gibin.** 2000. Survey of filamentous microorganisms from bulking and foaming activated-sludge plants in Italy. Water Res. **34:**1767–1772.
42. **McCarthy, A. J., and S. T. Williams.** 1992. Actinomycetes as agents of biodegradation in the environment—a review. Gene **115:**189–192.
43. **McCarthy, G. W.** 1999. Modes of action of nitrification inhibitors. Biol. Fertil. Soils **29:**1–9.
44. **Mobarry, B., M. Wagner, V. Urbain, B. Rittmann, and D. Stahl.** 1996. Phylogenetic probes for analyzing abundance and spatial organization of nitrifying bacteria. Appl. Environ. Microbiol. **62:**2156–2162.
45. **Muyzer, G., E. C. de Waal, and A. Uitterlinden.** 1993. Profiling of complex microbial populations using denaturing gradient gel electrophoresis analysis of polymerase chain reaction-amplified genes coding for 16S rRNA. Appl. Environ. Microbiol. **59:**695–700.
46. **Muyzer, G., and K. Smalla.** 1998. Application of denaturing gradient gel electrophoresis (DGGE) and temperature gradient gel electrophoresis (TGGE) in microbial ecology. Antonie Leeuwenhoek **73:**127–141.
47. **Nielsen, J. L., L. H. Mikkelsen, and P. H. Nielsen.** 2001. *In situ* detection of cell surface hydrophobicity of probe-defined bacteria in activated sludge. Water Sci. Technol. **43:**97–103.
48. **Nubel, U., B. Engelen, A. Felske, J. Snaidr, A. Wieshuber, R. I. Amann, W. Ludwig, and H. Backhaus.** 1996. Sequence heterogeneities of genes encoding 16S rRNAs in *Paenibacillus polymyxa* detected by temperature gradient gel electrophoresis. J. Bacteriol. **178:**5636–5643.
49. **Øvreas, L., L. Forney, F. L. Daae, and V. Torsvik.** 1997. Distribution of bacterioplankton in meromictic lake Saelevannet, as determined by denaturing gradient gel electrophoresis of PCR-amplified gene fragments coding for 16S rRNA. Appl. Environ. Microbiol. **63:**3367–3373.
50. **Purkhold, U., A. Pommerening-Roser, S. Juretschko, M. C. Schmid, H. P. Koops, and M. Wagner.** 2000. Phylogeny of all recognized species of ammonia oxidizers based on comparative 16S rRNA and amoA sequence analysis: Implications for molecular diversity surveys. Appl. Environ. Microbiol. **66:** 5368–5382.
51. **Rainey, F. A., N. L. WardRainey, P. H. Janssen, H. Hippe, and E. Stackebrandt.** 1996. *Clostridium paradoxum* DSM 7308(T) contains multiple 16S rRNA genes with heterogeneous intervening sequences. Microbiology **142:** 2087–2095.
52. **Spain, J. C., C. A. Pettigew, and B. E. Haigler.** 1991. Biodegradation of mixed solvents by a strain of *Pseudomonas.* Plenum Press, New York, N.Y.
53. **Suwa, Y., Y. Imamura, T. Suzuki, T. Tashiro, and Y. Urushigawa.** 1994. Ammonia-oxidizing bacteria with different sensitivities to $(NH_4)_2SO_4$ in activated sludges. Water Res. **28:**1523–1532.
54. **Suzuki, M., and S. Giovannoni.** 1996. Bias caused by template annealing in the amplification of mixtures of 16S rRNA genes by PCR. Appl. Environ. Microbiol. **62:**625–630.
55. **Vallaeys, T., E. Topp, G. Muyzer, V. Macheret, G. Laguerre, A. Rigaud, and G. Soulas.** 1997. Evaluation of denaturing gradient gel electrophoresis in the detection of 16S rDNA sequence variation in rhizobia and methanotrophs. FEMS Microbiol. Ecol. **24:**279–285.
56. **van Elsas, J. D., G. F. Duarte, A. S. Rosado, and K. Smalla.** 1998. Microbiological and molecular biological methods for monitoring microbial inoculants and their effects in the soil environment. J. Microbiol. Methods **32:** 133–154.
57. **Villaverde, S., F. Fdz-Olanco, and P. A. Garcia.** 2000. Nitrifying biofilm acclimation to free ammonia in submerged biofilters. Water Res. **34:**602–610.
58. **Wagner, M., R. Amann, P. Kaempfer, B. Assmus, A. Hartmann, P. Hutzler, N. Springer, and K. H. Schleifer.** 1994. Identification and *in situ* detection of Gram-negative filamentous bacteria in activated sludge. Syst. Appl. Microbiol. **17:**405–417.
59. **Wagner, M., R. Amann, H. Lemmer, and K. H. Schleifer.** 1993. Probing activated sludge with oligonucleotides specific for proteobacteria: inadequacy of culture-dependent methods for describing microbial community structure. Appl. Environ. Microbiol. **59:**1520–1525.
60. **Wanner, J., I. Ruzickova, P. Jetmarova, O. Krhutkova, and J. Paraniakova.** 1998. A national survey of activated sludge separation problems in the Czech Republic: Filaments, floc characteristics and activated sludge metabolic properties. Water Sci. Technol. **37:**271–279.

Downloaded from http://aem.asm.org/ on October 23, 2019 by guest